Determination of type I phase matching angles and conversion efficiency in KTP

M. H. van der Mooren, Th. Rasing, and H. J. A. Bluyssen

Measurements of the conversion efficiency of second-harmonic generation in KTP ($KTiOPO_4$) by the use of type I phase matching for different fundamental wavelengths of a mode-locked picosecond Ti:sapphire laser are presented. The observed phase matching angles are in agreement with the calculated phase matching curves. At a fundamental wavelength of 834 nm and an intensity of 100 MW/cm^2 the conversion efficiency is 4% at maximum, and the corresponding effective nonlinear coefficient d_{eff} is equal to 0.32 pm/V. The experimental values of d_{eff} are related to d_{11} (= 0.46 pm/V) of quartz and are in line with the predictions.

Key words: Type I phase matching, second-harmonic generation, KTP.

1. Introduction

KTP ($KTiOPO_4$) is a well-known nonlinear optical material[1] and is generally used as a second-harmonic generator for the 1064-nm radiation of a Nd:YAG laser. The conversion to second-harmonic generation is very efficient (up to 80%) when type II phase matching (PM) is used, but this technique is not possible[2] for wavelengths less than 990 nm. It has been shown theoretically[3] that type I PM is possible down to 740 nm with an effective nonlinear coefficient d_{eff} that is at least one order of magnitude smaller than for type II PM. Because of the high peak intensities that are available with a Ti:sapphire laser (720–860 nm) it can be expected that the laser's wavelength range can be frequency doubled by the use of type I PM with a reasonable efficiency. Second-harmonic generation by the use of type I PM in bulk KTP is an important experiment because it is a way to check the calculated d_{eff}. From the definition of the d_{eff} it can be seen that its value is mainly determined by the difference of two (almost equal) nonlinear optical tensor elements, d_{15} and d_{24}. When we include Kleinman's conjecture, it can be seen that d_{eff} is given by[4,5]:

$$\begin{aligned} d_{eff} = {} & 0.5(d_{24} - d_{15})\sin 2\theta \sin 2\phi(3\sin^2\delta - 1)\cos\delta \\ & + 3(d_{15}\cos^2\phi + d_{24}\sin^2\phi)\sin\theta\cos^2\theta\sin\delta\cos^2\delta \\ & + (d_{15}\sin^2\phi + d_{24}\cos^2\phi)\sin\theta\sin\delta(3\sin^2\delta - 2) \\ & + d_{33}\sin^3\theta\sin\delta\cos^2\delta, \end{aligned} \quad (1)$$

where δ is the angle between the polarization direction and the bisector of the optical axes. The angles θ and ϕ define the beam propagation direction with respect to the z and x axes of the crystal, respectively. We present conversion-efficiency measurements of a picosecond mode-locked Ti:sapphire laser at a fundamental beam intensity of 100 MW/cm^2 as a function of crystal orientation in flux-grown KTP[6] for fundamental wavelengths varying from 773 to 834 nm. To compare the calculated PM angles and d_{eff} with the experimental values, we give the transformation of the external measured phase match angles to the corresponding angles with respect to the crystal axes. Finally the importance of parameters such as the walk-off angle and angular acceptance is illustrated.

2. Experimental

The output of the picosecond mode-locked Ti:sapphire laser with pulse duration of 1 to 2 ps and a repetition rate of 82 MHz is controlled by a variable attenuator that consists of a Soleil Babinet compensator and a polarizer and is continuously monitored with a Scientech power detector and autocorrelator.

The authors are with the Research Institute for Materials, University of Nijmegen, Toernooiveld, Nijmegen 6525 ED, The Netherlands.

Received 20 July 1994; revised manuscript received 15 July 1994.
0003-6935/95/060934-04$06.00/0.

A vertically polarized laser beam with an average power of 0.6 W and a beam diameter of 1.6 mm is focused by a 160-mm lens to a focal spot diameter of 65 μm into a 4.75-mm-thick KTP crystal. In this way a typical intensity of 100 MW/cm^2 is reached for each wavelength. A diagram of the apparatus can be found in Ref. 4. The PM curves in Fig. 1 are calculated from the Fresnel equation and the Sellmeier equations for flux-grown KTP.[7] The PM angles and the values of the nonlinear coefficients of KTP[8] are substituted in Eq. (1) and are plotted as curves in Fig. 2. The crystal is cut for the maximum value of d_{eff} at 800 nm, which is approximately the middle of the wavelength range of the available Ti:sapphire laser. From the curves in Figs. 1 and 2 it can be seen that the beam propagation direction for PM at 800 nm for maximum d_{eff} is $(\theta, \phi) = (70°, 50°)$. In Fig. 3 the crystal axes are denoted by x, y, z, and the laboratory frame is denoted by u, v, w. The v axis is perpendicular to the saw plane, and the direction of the v axis with respect to the crystal axes is defined by two rotations carried out to cut the crystal perpendicular to the original y axis:

$$\begin{bmatrix} \cos\theta_c & 0 & -\sin\theta_c \\ 0 & 1 & 0 \\ \sin\theta_c & 0 & \cos\theta_c \end{bmatrix} \begin{bmatrix} \cos\phi_c & \sin\phi_c & 0 \\ -\sin\phi_c & \cos\phi_c & 0 \\ 0 & 0 & 1 \end{bmatrix} \begin{pmatrix} 0 \\ 1 \\ 0 \end{pmatrix}, \quad (2)$$

where $\theta_c = 90° - 70°$ and $\phi_c = 90° - 50°$ are the cutting angles. The u direction is chosen as the cross section of the (201) plane and the saw plane. The relation between the laboratory system and the crystal system is known and can be given by a transformation matrix A [A is the matrix in Eq. (4), below, where u_x is the x component of u, etc.]. The crystal orientation was checked, and it agreed within the accuracy of the Laue method ($\pm 1°$) that we used.

The conversion efficiency follows from the ratio of the blue and red peak powers and was determined as a function of the rotation angles α and β around the u and w axes, respectively, for different wavelengths. The difference in detector sensitivity at the red and blue wavelengths is less than 3%. The accuracy of the angle positioning is 0.01° for β and 0.1° for α. Varying β gives us a maximum for the generated second harmonic at a certain fixed α. For each wavelength a curve of (α, β) points for which PM takes place was measured. These curves were published in Ref. 4.

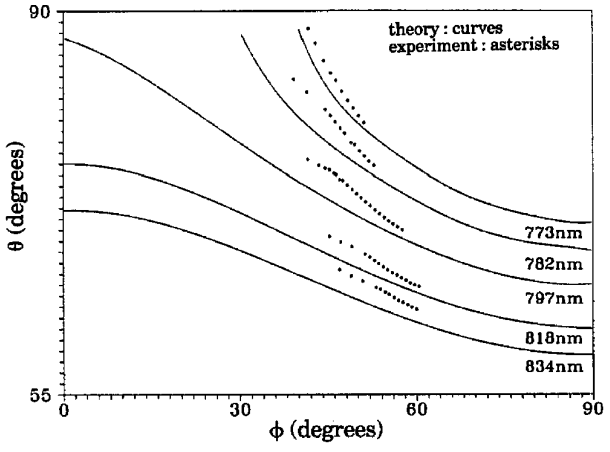

Fig. 1. KTP PM curves for type I second-harmonic generation.

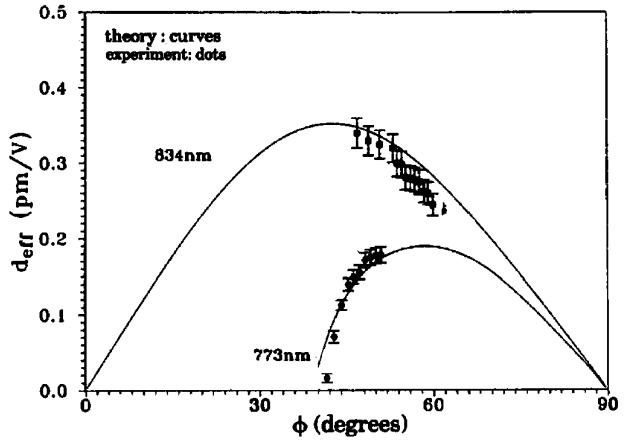

Fig. 2. Calculated (curves) and measured (dots) d_{eff} as a function of the PM angle ϕ. Each value of ϕ corresponds to a particular θ value according to Fig. 1.

3. Results

3.A. Phase Matching Angles

To compare experiment with theory, we transform the measured (α, β) to crystal angles (ϕ, θ). This transformation is described below. Normal incidence means that the beam is parallel to the v direction. In general the direction of the incident beam $\mathbf{i}$ is a function of the angles α and β according to rotation multiplication in matrix notation:

$$\mathbf{i} = \begin{bmatrix} \cos\beta & \sin\beta & 0 \\ -\sin\beta & \cos\beta & 0 \\ 0 & 0 & 1 \end{bmatrix} \begin{bmatrix} 1 & 0 & 0 \\ 0 & \cos\alpha & -\sin\alpha \\ 0 & \sin\alpha & \cos\alpha \end{bmatrix} \begin{pmatrix} 0 \\ 1 \\ 0 \end{pmatrix}. \quad (3)$$

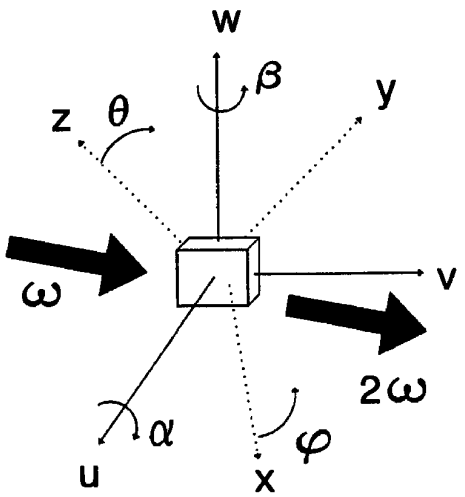

Fig. 3. Laboratory frame u, v, w and angles α and β. Also shown are crystal axes x, y, z and angles ϕ and θ.

Multiplying the transformation matrix A by the result of Eq. (3) gives us $\mathbf{i}$ with respect to the crystal axes:

$$\mathbf{i} = \begin{bmatrix} u_x & v_x & w_x \\ u_y & v_y & w_y \\ u_z & v_z & w_z \end{bmatrix} \begin{pmatrix} \cos\alpha \sin\beta \\ \cos\alpha \cos\beta \\ \sin\alpha \end{pmatrix}. \quad (4)$$

The angle of incidence is defined by the scalar product of $\mathbf{i}$ and the unit vector $\mathbf{v}$. From Snell's law the refraction angle r is obtained by the use of iteration, because the refraction index n depends on the refraction angle:

$$r = \arcsin[\sin[\arccos(\mathbf{i} \cdot \mathbf{v})]/n(r)]. \quad (5)$$

The angle r is also equal to the scalar product of $\mathbf{r}$ and $\mathbf{v}$, where the refracted beam $\mathbf{r}$ lies in the plane of incidence. The PM angles are obtained from

$$\theta = \arccos(r_z),$$
$$\phi = \arctan(r_y/r_x). \quad (6)$$

The results of these calculations are plotted in Fig. 1. Apart from a small shift in the upper direction the PM angles are in good agreement with the calculated PM curves. Possible explanations for the observed shift are, first, a systematic error that is due to a small orientation error and, second, the calculated PM curves are based on empirical data from Ref. 7. The fourth decimal of the refraction index is significant for the determination of the PM angles. The growth conditions are different for each process, and this can be seen, for instance, in a significant difference in ionic conductivity, and therefore a slight difference in the refraction index can be expected.

3.B. Effective Nonlinear Coefficient and Conversion Efficiency

To determine the conversion efficiency it is necessary to know which fraction of the incident power is convertible. The polarization direction is kept fixed along the vertical direction, and the convertible fraction is given by the scalar product of the unit vector of the electric-field direction in the crystal with the convertible component of the polarization direction, which is defined by[5]

$$\begin{pmatrix} \cos\theta \cos\phi \cos\delta - \sin\phi \sin\delta \\ \cos\theta \sin\phi \cos\delta + \cos\phi \sin\delta \\ -\sin\theta \cos\delta \end{pmatrix}. \quad (7)$$

Taking the Fresnel losses into account, we found the maximum efficiency at 834 nm to be 4.2%. The efficiency curves for different wavelengths as a function of the PM orientation are shown in Fig. 4.

From the small signal approximation for the conversion efficiency[9] and the reference measurement of $d_{11} = 0.46$ pm/V of quartz,[9] the experimental value of d_{eff} was obtained. The results for d_{eff} values of 834 and 773 nm are plotted in Fig. 2 and show the same dependence as the calculated values. The substituted nonlinear coefficients in Eq. (1) in picometers per volt are $d_{15} = -1.85$, $d_{24} = -4.31$, and $d_{33} = -17.2$, and these values are within the error margins of the reported values.[8] At 834 nm these values give us, after substitution, a d_{eff} of 0.07 pm/V at maximum, where the above-mentioned values result in a d_{eff} of 0.35 pm/V (see Fig. 2). The large uncertainty in the calculated d_{eff} mainly is due to the inaccuracy of the difference between d_{15} and d_{24}. The absolute values of the measured d_{eff} depend on the d_{11} of the quartz that was used. For instance the d_{11} used in Ref. 8 (= 0.31 pm/V) will result in lower values for d_{eff}, and correspondingly other nonlinear coefficients are needed to fit the experimental data. When we look at the curves in Fig. 2 and compare the results of the two wavelengths, the magnitudes of d_{eff} at 773 nm generally fall above and those at 834 nm fall below the calculated curves. Possible explanations for this difference are, first, the walk-off angle, which limits the interaction length, and second, the values for the acceptance angles that are of the same magnitude as the focusing geometry. The walk-off angle is calculated to be more than 2° above 800 nm and for PM orientations with ϕ greater than 50°. Irrespective of the PM orientation, below 800 nm the walk-off angle is less than 2°. The calculated bandwidth[10] for ϕ for all wavelengths used is at least 25 mm mr. The beam that is incident upon the crystal has a divergence of 4.5 mr. Therefore a crystal of 4.75-mm thickness accepts all incident angles in the x, y plane. For wavelengths larger than 800 nm the acceptance for θ is smaller than 21 mm mr, and for smaller wavelengths the acceptance depends strongly on the PM angle. At 773 nm the acceptance is between 22 and 15 mm mr for the PM orientations used. For a type I cut crystal it is difficult to say whether the external angular bandwidth is large enough because the beam propagation is not in a principal plane. Given the experimental circumstances and the angular bandwidth and walk-off calculations, it is clear

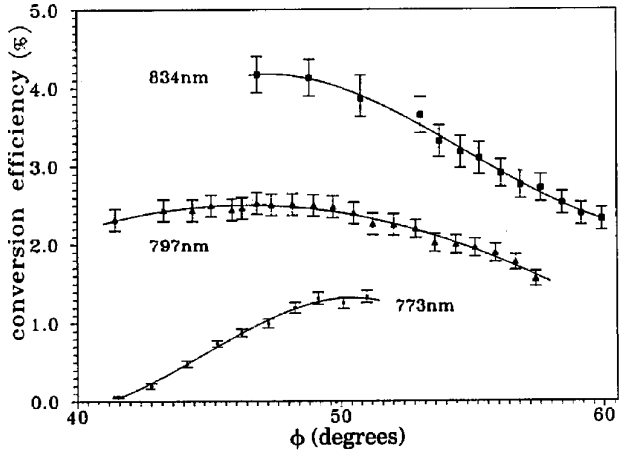

Fig. 4. Experimentally determined conversion efficiency for different wavelengths as a function of the PM orientation.

that the situation for optimal conversion at 773 nm is far less critical than at 834 nm. Finally it should be mentioned that the spectral bandwidth[10] of the crystal is large enough (6 mm nm) for the crystal to accept the spectral range of the incident pulse, which is 0.5 nm for a 2-ps Gaussian pulse.

4. Conclusion

We have shown that second-harmonic type I PM in bulk KTP is experimentally possible, and the above-determined PM angles agree well with the calculated values. At 834 nm the maximum measured conversion efficiency is 4%. The experimental values of d_{eff} show the same dependence as the calculated curves, which are strongly dependent on the factor $d_{15} - d_{24}$.

The authors thank P. C. M. Christianen, C. A. van't Hof, A. F. van Etteger, and R. J. Bolt for all kinds of help. M. H. van der Mooren acknowledges the financial support of Stichting voor Technische Wetenschappen.

References

1. F. C. Zumsteg, J. D. Bierlein, and T. E. Gier, "$K_xRb_{1-x}TiOPO_4$: a new nonlinear material," J. Appl. Phys. **47,** 4980–4985 (1976).
2. D. W. Anthon and C. D. Crowder, "Wavelength dependent phase matching in KTP," Appl. Opt. **27,** 2650–2652 (1988).
3. J. Q. Yao and T. S. Fahlen, "Calculation of optimum phase match parameters for the biaxial crystal $KTiOPO_4$," J. Appl. Phys. **55,** 65–68 (1984).
4. M. H. van der Mooren, Th. Rasing, and H. J. A. Bluyssen, "Second harmonic generation of blue light in bulk KTP by type I phase matching," in *Proceedings of the International Conference on Lasers '92,* C. P. Wang, ed. (STS, McLean, Va., 1993), pp. 264–267.
5. H. Ito, H. Naito, and H. Inaba, "Generalized study on angular dependence of induced second order nonlinear optical polarizations and phase matching in biaxial crystals," J. Appl. Phys. **46,** 3992–3998 (1975).
6. R. J. Bolt, M. H. van der Mooren, and H. de Haas, "Growth of $KTiOPO_4$ (KTP) single crystals by means of phosphate and phosphate/sulfate fluxes out of a three-zone furnace," J. Cryst. Growth **114,** 141–152 (1991).
7. T. Y. Fan, C. E. Huang, B. Q. Hu, R. C. Eckardt, Y. X. Fan, R. L. Byer, and R. S. Feigelson, "Second harmonic generation and accurate index of refraction measurements in flux-grown $KTiOPO_4$," Appl. Opt. **26,** 2390–2394 (1987).
8. H. Vanherzeele and J. D. Bierlein, "Magnitude of the nonlinear-optical coefficients of $KTiOPO_4$," Opt. Lett. **17,** 982–984 (1992).
9. A. Yariv, *Quantum Electronics,* 2nd ed. (Wiley, New York, 1975), Chap. 16, pp. 416 and 431.
10. J. Yao, W. Sheng, and W. Shi, "Accurate calculation of the optimum phase-matching parameters in three-wave interactions with biaxial nonlinear-optical crystals," J. Opt. Soc. Am. B **9,** 891–902 (1992).